Volume 3, Issue 10, October - 2025 **ISSN (E):** 2938-3811

# INTEGRATION OF GENETIC ALGORITHM WITH SLEUTH FOR URBAN GROWTH MODELING IN AL-SULAYMANIYAH CITY, NORTHERN IRAQ

Nyan Qasim Khudhur 1
Dler A. Al-Mamany 2
1 Northern Technical University, Surveying Eng. Techniques Dept.,
Email: nyan.qasimgs@ntu.edu.iq
2 Northern Technical University, Surveying Eng. Techniques Dept.,
Email: dlieromer@ntu.edu.iq

**Abstract**
This work introduces a novel fusion of genetic algorithm (GA) optimization with the SLEUTH cellular automaton model to simulate and forecast urban growth dynamics in Al-Sulaymaniyah City, Kurdistan Region, Iraq. To overcome the computational constraints of conventional SLEUTH calibration, we devised a GA-based optimization framework that attained a 3-22x acceleration while preserving good accuracy. The GA optimization effectively calibrated the SLEUTH growth coefficients, achieving an Optimal SLEUTH Metric of 0.718±0.16 and a Lee-Sallee index of 0.900±0.05. Model validation revealed a continuous increase in accuracy from 83.45% in 2004 to 91.27% in 2024, signifying an improved ability to capture modern urban dynamics. Projections for 2034 anticipate a total urban area of 878.20 km², indicating a 511.1% increase from the 1995 baseline. Spatial analysis indicated a significant northwestern directional bias (549% increase) and a diminishing connection with road proximity over time (r = -0.188 to -0.073), implying a transition from infrastructure-dependent to multi-factor-driven urban expansion. The model delineated specific growth phases: a period of rapid expansion (1995-2010) averaging 23.84 km²/year, succeeded by a reduction to 5.79 km²/year (2020-2034), signifying impending geographical saturation. The SLEUTH-GA framework offers urban planners quick and precise tools for simulating intricate urban systems and developing evidence-based sustainable policies in swiftly expanding Middle Eastern cities.

**Keywords**: Urban Growth Modeling, Genetic Algorithm, SLEUTH Model, Calibration.

## Introduction

Accelerated urbanization in emerging cities poses significant problems for sustainable development planning, requiring advanced modeling techniques that can precisely forecast future growth trends and guide evidence-based policy decisions in data-scarce contexts [1]. The SLEUTH (Slope, Land use, Exclusion, Urban, Transportation, Hillshade) cellular automata model has become a prevalent instrument for spatially explicit urban growth







Web of Scientists and Scholars: Journal of Multidisciplinary Research

simulation, effectively utilized in various geographic settings from European cities to Asian megacities; however, its conventional brute-force calibration method is still computationally demanding and time-consuming [2], [3]. Genetic algorithms significantly enhance SLEUTH modeling by substituting the traditional multi-phase calibration process with an evolutionary optimization method, resulting in a 3-22x increase in computational speed, improved parameter optimization accuracy, and the removal of human subjectivity in calibration [4]. Al-Sulaymaniyah City in Northern Iraq serves as a notable case study for sophisticated urban growth modeling, having undergone significant transformation with a 61% population increase from 1991 to 2018 due to political autonomy and post-conflict reconstruction. This has resulted in distinctive urban dynamics influenced by substantial internal migration, oil revenue development, and the challenges of integrating over 260,000 displaced individuals within a swiftly expanding urban environment [5]. The SLEUTH model, which integrates slope, land use, exclusion zones, urban areas, transportation, and hillshade, effectively simulates urban expansion situations. It utilizes cellular automata concepts in conjunction with historical data for thorough urban growth forecasts [6], [7]. Although the model has been successfully implemented in areas such as Japan and other regions of the U.S., there is a lack of direct studies concentrating on Al-Sulaymaniyah, despite the technological feasibility of adapting this framework [8]. Recent investigations have utilized genetic algorithms to improve the forecasting efficacy of the SLEUTH urban growth model. These initiatives generally emphasize enhancing calibration processes, wherever genetic algorithms supplant conventional brute-force techniques, refine parameter selection, and elevate the model's predicted accuracy [8]. While these strategies have been effectively implemented in several global regions, tangible evidence of their integration in Al-Sulaymaniyah, northern Iraq, remains scarce.

Research in Al-Sulaymaniyah has mostly employed Cellular Automata Markov (CA-Markov) models to forecast urban growth with satellite imagery. These studies have delineated urban expansion from 1991 to 2014 [9]. The current body of research indicates a fundamental comprehension of urban dynamics in the region that could be augmented by genetic-algorithm-enhanced SLEUTH applications. Considering the technical improvements, there exists considerable potential to further investigate the synergy between genetic algorithms and SLEUTH in the context of Al-Sulaymaniyah. Such studies could provide enhanced urban growth forecasts that consider the region's distinct socio-spatial attributes. Existing approaches employed in analogous urban situations provide viable avenues for implementation in Kurdish and Iraqi environments [10], [11].

Genetic algorithms (GAs) markedly improve urban growth prediction models by optimizing intricate parameter spaces. They facilitate efficient calibration and scenario analysis by determining ideal coefficient settings in models such as SLEUTH, which encompass characteristics including dispersion, breed, spread, slope, and road gravity [12]. This optimization is essential as conventional calibration techniques can be computationally demanding and may neglect nuanced interdependencies among parameters, particularly in diverse urban configurations [6]. Moreover, GAs provide multi-objective optimization, hence

augmenting the models' ability to accurately replicate fragmented and varied urban growth patterns [13]. For instance, they provide integrated methodologies that merge cellular automata with neural networks or Markov chains, hence enhancing prediction precision in urban growth contexts [12].

The SLEUTH model, while widely utilized, encounters numerous obstacles in forecasting urban expansion. The model encounters difficulties in accurately representing minor, dispersed urban developments, especially in areas characterized by fragmented or informal urbanization patterns [7]. Calibration is intricate and resource-demanding, necessitating meticulous parameterization to prevent substantial prediction inaccuracies. The self-adjusting parameters, essential for modeling nonlinear urban processes, necessitate careful calibration. The precision of forecasts is significantly influenced by the quality and resolution of input data, including land cover maps, transportation networks, and exclusion layers. Insufficient representation may result in implausible growth projections. SLEUTH successfully utilizes physical and infrastructural data; nevertheless, it frequently neglects dynamic socioeconomic elements such as migration trends and economic conditions, hence constraining its comprehensive forecasting capacity [14].

The principal objective of employing urban development prediction models such as SLEUTH, augmented by genetic algorithms, is to precisely anticipate urban expansion trends, evaluate their effects on land utilization, and facilitate sustainable urban planning. Specific objectives generally encompass

- Employing satellite and GIS data to monitor and assess alterations in urban, agricultural, and natural landscapes across time.
- Ensuring that models appropriately represent past growth trends and comply with validation metrics, including the Optimal SLEUTH Metric (OSM).
- Examining the influence of infrastructural components, like roadways and regulatory limitations, on urban development.

## 2. LITERATURE REVIEW

The SLEUTH model, created by Clarke and associates in the 1990s, functions as a self-modifying cellular automaton that mimics four primary forms of urban expansion: spontaneous growth, diffusive growth, organic growth, and road-influenced growth [15]. The model's theoretical framework is based on five essential growth coefficients—diffusion, breed, spread, slope resistance, and road gravity—that govern growth probabilities across gridded spatial data layers [16]. The coefficients span from 0 to 100 and interact in intricate, non-linear manners to generate emergent patterns of urban growth [16]. Conventional SLEUTH calibration utilized a resource-intensive "brute force" approach that methodically examined all potential parameter combinations through three successive stages: coarse, fine, and final calibration [16]. This methodology necessitated between 59,375 and 71,875 separate Monte Carlo simulation executions for comprehensive calibration, utilizing hundreds of thousands of CPU hours and frequently demanding years to analyze intricate datasets [2], [17]. The brute force method exhibited significant limitations, such as computational intractability for extensive datasets,

reliance on subjective human input for parameter selection, and the possibility of failing to discover globally optimal parameter combinations due to its exhaustive yet sequential search methodology [4]. Parameter sensitivity research identified further issues, as SLEUTH coefficients demonstrate intricate interdependencies that fluctuate according on geographic context, spatial resolution, and temporal calibration periods [7]. The conventional method frequently led to overfitting, wherein statistically ideal parameters generated spatially implausible growth patterns, underscoring the necessity for more advanced calibration techniques. The combination of genetic algorithms with SLEUTH calibration signifies a transition from exhaustive search methods to evolutionary optimization techniques. Genetic algorithms substitute exhaustive parameter exploration with population-based search strategies that develop optimal parameter combinations via selection, crossover, and mutation processes [10]. Within the GA-SLEUTH framework, each chromosome encompasses the five SLEUTH growth parameters, and populations ranging from 18 to 40 chromosomes evolve across 5 to 200 generations to ascertain appropriate calibration solutions. The GA implementation employs the Optimal SLEUTH Metric (OSM) as its principal fitness function, which encapsulates a composite assessment of seven calibration criteria: compare coefficient, population coefficient, edges coefficient, clusters coefficient, slope coefficient, and spatial fit measures [18]. This method removes subjective human parameter selection, offering mathematical objectivity in calibration optimization. The genetic algorithm utilizes advanced selection methods, such as tournament selection and elitism preservation, alongside uniform and self-crossover procedures to sustain population variety while retaining high-performing solutions [2].

Advancements in technical implementation have rendered GA-SLEUTH entirely automated, necessitating minimal human participation while attaining calibration quality that is superior or similar to conventional approaches. The algorithm employs adaptive mutation rates, parameter-specific crossover techniques, and incremental increases in Monte Carlo iterations (4, 5, 10, 15, and 20 runs) to optimize computational efficiency and statistical robustness. The computational benefits of GA-SLEUTH integration are significant and thoroughly documented in many comparison studies [4]. Research regularly shows calibration performance that is 3-22 times faster than brute force approaches, decreasing calibration time from years to days for intricate urban datasets [10]. This significant enhancement in efficiency arises from the evolutionary search approach, which navigates parameter space more intelligently than exhaustive enumeration [17]. The comparative analysis conducted by Saxena and Jat [7] in Ajmer, India, revealed that GA calibration not only attained enhanced computational efficiency but also yielded improved urban growth pattern representation and elevated Kappa statistics in comparison to conventional approaches. Likewise, Jafarnezhad et al. [18] confirmed the superiority of GA in three Iranian cities—Azadshahr, Gonbadekavoos, and Gorgan—demonstrating consistent enhancements in landscape measures. The GA technique mitigates significant drawbacks of conventional calibration by circumventing local optima traps via a population-based search and preserving solution variety through genetic operators. Validation studies utilize various accuracy assessment methods, such as Kappa coefficients (generally

exceeding 0.80 for satisfactory outcomes), Lee-Sallee spatial fit indices (acceptable performance within the 0.3-0.7 range), and overall classification accuracies between 85-95% [19]. The study of spatial accuracy with Figure of Merit (FoM) metrics indicates that SLEUTH attains a FoM value of 0.26 in comparative analyses, while landscape metrics offer pattern-based confirmation for growth forecasts.

Significant regional applications illustrate the model's versatility across many metropolitan environments. In China, extensive applications encompass Hefei [14], Shenyang [20], Wuhan [14], and Beijing[21], demonstrating successful calibration and validation across various urban development patterns and growth rates. Indian applications in Prayagraj [6] and Pune exhibit efficacy in the setting of rapidly expanding urban environments, with yearly growth rates of 1.9% precisely documented and forecasted. The foundational Lisbon and Porto studies [16] initiated European applications that demonstrated model universality beyond North American contexts. Turkish applications in Adana [19] attained a Kappa accuracy of 75%, the highest among evaluated cellular automata models, illustrating SLEUTH's efficacy in Mediterranean metropolitan settings characterized by significant development unpredictability. African applications provide solid evidence of model adaptability in emerging country situations. Nigerian studies focusing on Kano, Katsina, Kaduna, and other northern cities [22] demonstrated that larger cities with dense settlement patterns attained greater prediction accuracy, with Lee-Sallee values varying from 0.02 to 0.83 based on urban morphology and scale attributes.

## 3. METHODOLOGY

### 3.1 Study Area

Al-Sulaymaniyah City, situated in the Kurdistan Region in northern Iraq, serves as a significant metropolitan hub both demographically and culturally. The city is located in a complicated topography surrounded by substantial topographical barriers, rendering it an intriguing subject for urban growth modeling (Figure 1). Al-Sulaymaniyah has experienced significant and continuous urban growth in recent decades [9]. From 1991 to 2014, developed land expanded from 13.3% (3,063.78 hectares) to 41.8% (9,654.26 hectares), indicative of population pressure and economic advancement. The city is considered the cultural capital of Kurdistan, with a demographic growth of roughly 3% per annum. In 1987, 63% of the population resided in urban areas, a proportion that increased to 78% by 2008, reflecting significant urban expansion [9]. The catalysts of this urbanization encompass substantial economic advancements post-2003 and an escalation in construction across all sectors, including residential, commercial, educational, and infrastructural. The expansion has occurred at the cost of agricultural and open lands, resulting in significant alterations to the city's land use and land cover structure. The city's alterations render it an exemplary testbed for urban modeling methodologies that account for nonlinear, spatially intricate growth processes, exemplified by SLEUTH and optimization-based calibrations such as Genetic Algorithms [9]. The urban expansion of Al-Sulaymaniyah is intricately linked to its transportation infrastructure. The city is situated in an inter-provincial junction, flanked by the Erbil and Kirkuk governorates to the west and southwest, and has an

eastern boundary with Iran [9]. The primary road system exhibits radial and circumferential patterns radiating from the city center to peripheral areas and adjacent towns. The proliferation along these transportation corridors is a characteristic hallmark of contemporary urban development, as construction has concentrated around primary highways and arterial routes owing to enhanced accessibility and economic prospects. The spatial link between urban expansion and the transportation network is a crucial component of modeling frameworks like SLEUTH, where road-influenced growth coefficients significantly influence projected spatial development [6]. The region is delineated by varied topography: the Baranan and Chwarta mountains to the south, the Tasluja hills to the west, and the Qaiwan range, Azmaer, and Goizha mountains to the north and northeast. This mountainous confinement results in considerable topographical limitations and microclimatic diversity throughout the city's growth area. The city displays a semi-arid climate characterized by hot, arid summers and cold, moist winters, which further affects settlement patterns and urban growth trajectories [9].

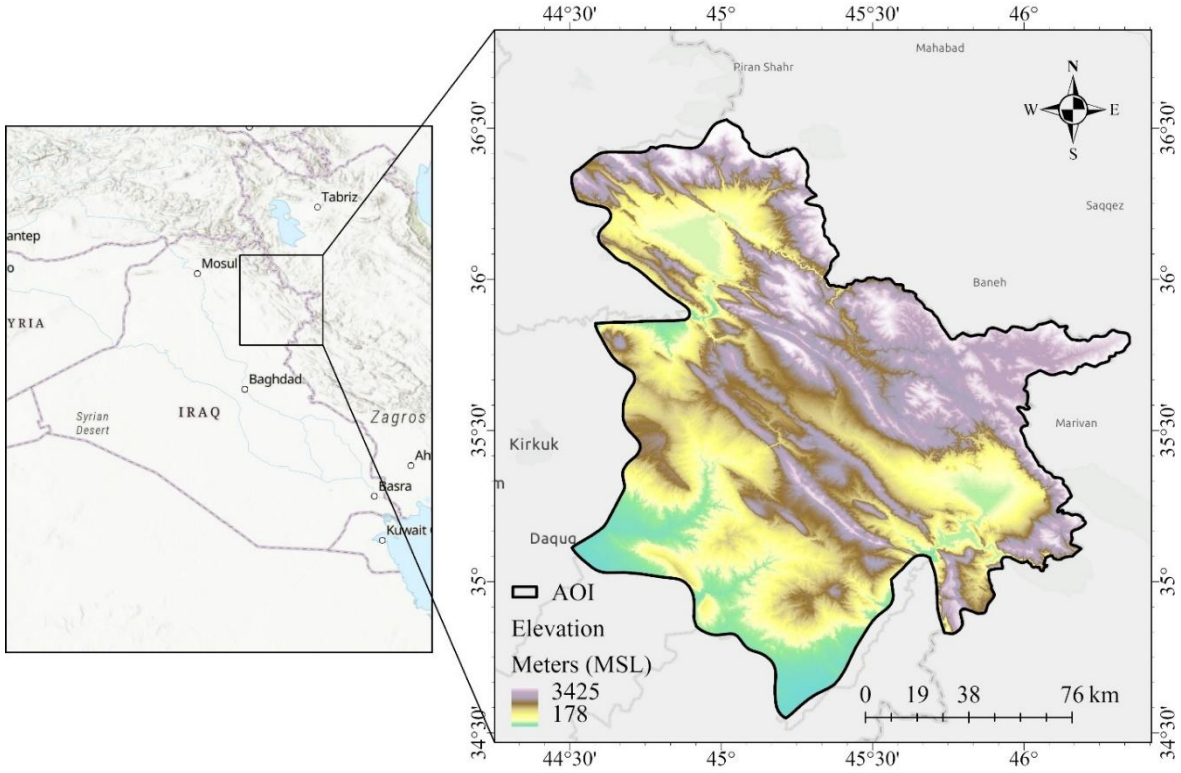


Figure 1. Map of the study area.

### 3.2 Datasets

#### 3.2.1 Preparation of the SLEUTH Exclusion Layer

The SLEUTH urban growth model necessitates an exclusion layer as a critical input to delineate regions where urbanization is entirely or partially constrained by environmental, legal, or planning limitations. The meticulous creation of this exclusion layer is essential for exact urban growth simulation and scenario analysis in spatial modeling. A range of geographic datasets is employed to delineate exclusion zones, each associated with particular land protections or usage restrictions (Figure 2). Table 1 delineates the standard datasets together

with their respective sources. Exclusion levels are established based on planning rules, management strategies, or scenario-specific parameters. The exclusion layer is formulated as a raster, wherein each pixel possesses a value that generally spans from 0 (completely available for urbanization) to 100 (entirely excluded from urbanization), indicating the likelihood or extent of exclusion. The preparation process encompasses multiple stages. Initially, the necessary vector and raster datasets are imported into the GEE environment. The datasets are subsequently projected into a unified coordinate reference system and resampled to the specified model resolution. Spatial buffers for features necessitating buffer zones (e.g., streams, wetlands) are created with geodesic buffering techniques in GEE. Subsequently, all vectors (e.g., polygons of protected areas) are transformed into raster format with the specified cell size. Each exclusion feature is allocated a threshold value that signifies the probability of exclusion. For instance, protected areas may be assigned a value of 100 (complete exclusion), whereas buffers surrounding streams may be allocated intermediate exclusion values (e.g., 60–80), contingent upon policy situations [23]. Subsequently, all individual exclusion rasters are amalgamated by cell-wise maximum or weighted sum processes, yielding a composite exclusion map. Overlapping regions are allocated the maximum exclusion value available. The composite exclusion raster is ultimately exported as a grayscale image (e.g., 8-bit GIF) to meet the spatial and format specifications of the SLEUTH model [6], [24].

Table 1. Summary of input layers, sources, and thresholds used to create the exclusion layer.

| Feature Type | Data Source | Buffer/Processing | Exclusion Value (%) |
|---|---|---|---|
| Protected Areas | WDPA, national shapefiles | None | 100 |
| Major Water Bodies | ESRI World Water Bodies, JRC, HydroSHEDS | 0–135m buffer | 60–100 |
| Farmland | ESA, National agricultural data | Parcels > defined acreage | 50/70–90 |
| Steep Slopes | SRTM DEM, GLOBE DEM | >21% gradient | 100 |
| Developed Areas | Landsat-based classification, LandScan | Urban pixels | 0 |







Web of Scientists and Scholars: Journal of Multidisciplinary Research

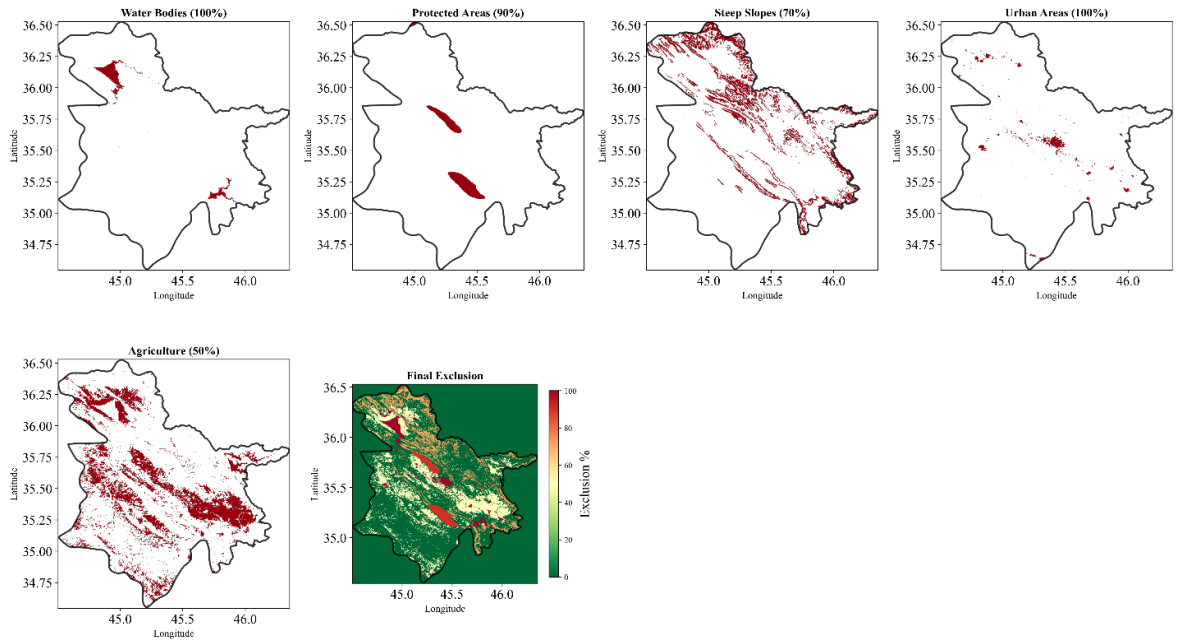


Figure 2. Exclusion layers and the final exclusion layer prepared from global datasets.

### 3.2.2 Land Cover

Land cover classification was performed with multitemporal Landsat imagery over a duration of three decades to assess terrain change. Landsat 5 Thematic Mapper (TM), Landsat 7 Enhanced Thematic Mapper Plus (ETM+), and Landsat 8 Operational Land Imager (OLI) images were obtained for the years 1994, 2004, 2014, and 2024, offering decadal insights into land cover transformation. Images were chosen during analogous phenological periods to mitigate seasonal fluctuation effects and achieve categorization uniformity throughout the temporal series. A seven-class land cover categorization scheme was established utilizing the Land Cover categorization System (LCCS) framework, which includes water, trees, flooded vegetation, crops, built environments, bare ground, and rangeland categories (Table 2). The training dataset comprised 50 polygon samples per class, with each polygon containing 10-50 pixels to encapsulate intra-class spectral diversity while preserving spatial homogeneity. Training polygons were delineated using visual analysis of high-resolution data and field expertise, guaranteeing representative sampling across varied landscape conditions within each category. Land cover classification using random forest (RF) learning techniques, capitalizing on the method's resilience to noise and its ability to manage high-dimensional spectral data. The RF classifier employed all available Landsat spectral bands, with training data divided into 70% for training and 30% for validation subsets by stratified random selection to preserve class proportionality. The model's performance was assessed using confusion matrices, overall accuracy metrics, and per-class producer's and user's accuracies to evaluate classification reliability over the temporal series.

Table 2. Land cover classification scheme based on the Land Cover Classification System (LCCS).

| Land Cover Class | Description |
|---|---|
| Water | Areas that are naturally or artificially covered by water for at least most of the year. These include natural lakes, rivers, reservoirs, and lagoons. |
| Trees | Areas dominated by woody vegetation consisting of trees whose height is generally greater than 5 meters, forming a continuous or open canopy. |
| Flooded Vegetation | Areas transitional between terrestrial and aquatic systems, where water is at or near the surface for a substantial period regularly every year. The predominant vegetation comprises hydrophytes, such as marshes, swamps, bogs, and mangroves. |
| Crops | Areas where the natural vegetation has been removed or modified and replaced by crops or other types of planted and cultivated vegetative cover. This includes annual and perennial crops, orchards, and plantations (rubber, palm oil, etc.), where vegetation is of anthropogenic origin and requires human activity to maintain it in the long term. |
| Built Area | Areas that have an artificial cover as a result of human activities such as construction (cities, towns, roads), extraction (mines), or waste disposal. These areas are dominated by impervious surfaces—such as asphalt, concrete, and buildings—with little or no natural vegetation. |
| Bare Ground | Areas with minimal to no vegetation (total vegetative cover less than 4% for more than 10 months of the year), including bare rock, sand, and deserts. These areas do not have a significant artificial cover and are characterized mainly by the appearance of the surface, whether consolidated or unconsolidated (rock, sand, or soil). |
| Rangeland | Areas dominated by natural or semi-natural herbaceous vegetation (graminoids and forbs) and occasionally shrubs, used primarily for livestock grazing and wildlife habitat. |

### 3.2.3 Road Networks

The development of historical road networks for the research area using a multi-source methodology that included archival geospatial data, remote sensing analysis, and manual digitization techniques. Historical OpenStreetMap (OSM) road data constituted the principal basis for modern road network extraction. Historical data from OSM was retrieved via the Overpass API, with filters applied for highway tags and temporal features relevant to the study period. The extracted vector data supplied foundational road geometry and attribute information, encompassing road classifications and temporal metadata wherever accessible. The Landsat satellite imagery relevant to the study's timeframe was meticulously examined to detect and digitize road features absent from current databases. Roads were manually digitized at suitable scales using Geographic Information Systems (GIS) software, through on-screen analysis of spectral properties and spatial patterns indicative of transportation routes. Extensive manual editing was conducted to maintain topological linkages, ensuring network connectivity and analytical validity. This procedure encompassed (1) geometric correction of digitized features to rectify overshoots, undershoots, and pseudo-nodes; (2) establishment of appropriate connectivity at road intersections; (3) validation of network topology utilizing GIS topology

rules; and (4) attribution of temporal parameters to individual road segments based on imagery analysis. The resultant historical road network database offers a geographically and temporally precise depiction of the history of transportation infrastructure, appropriate for SLEUTH modeling.

### 3.2.4 Terrain Analysis and Topographic Data Preparation

Terrain study utilized the Advanced Spaceborne Thermal Emission and Reflection Radiometer Global Digital Elevation Model (ASTER GDEM) version 3, which offers elevation data at a spatial resolution of 30 meters. The ASTER GDEM dataset provides large global coverage with vertical accuracy appropriate for regional topographic study and has undergone thorough validation for geomorphological applications. Hillshade and slope layers were generated from the ASTER GDEM utilizing the surface analysis capabilities in ArcGIS Pro (Figure 3). The hillshade layer was created using conventional illumination conditions, with an azimuth of 315° and a height of 45°, ensuring good observation of terrain relief and surface shape. The slope layer was determined as the highest rate of change between each cell and its adjacent cells, represented in degrees from the horizontal plane. The surface analysis tools utilized a 3×3 moving window approach to calculate local terrain derivatives, so maintaining spatial consistency throughout the study region.

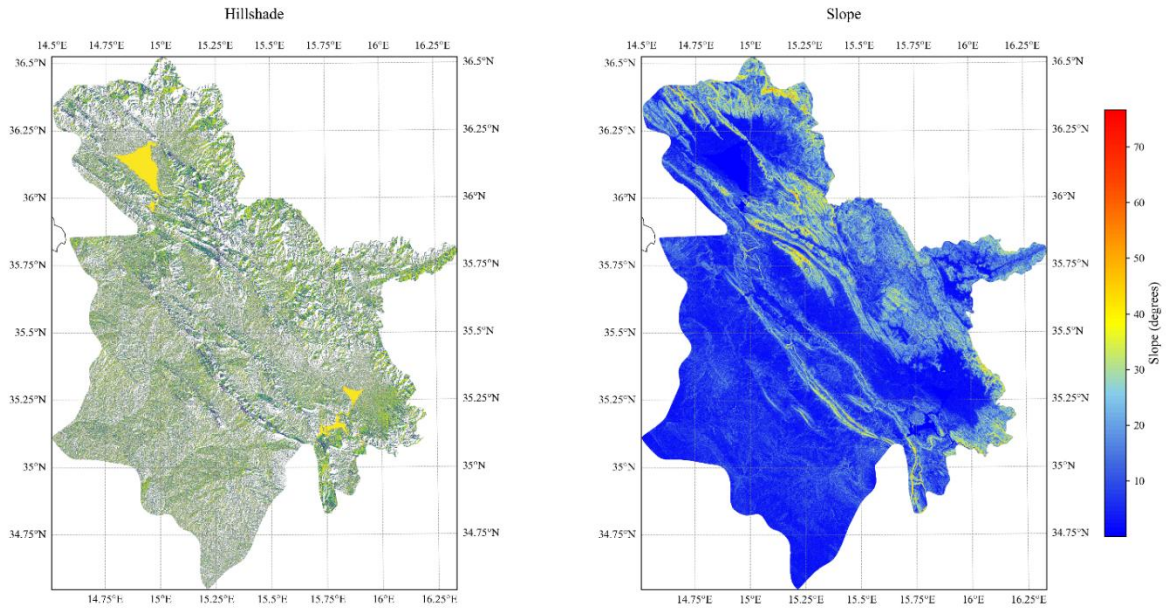


Figure 3. Maps of the hillshade and slope features.

### 3.3 Urban Growth Simulation Model

### 3.3.1 Genetic Algorithm

The Genetic Algorithm functions on a population of candidate solutions, with each individual embodying a distinct configuration of SLEUTH growth coefficients: Diffusion, Breed, Spread, Slope Resistance, and Road Gravity. Each parameter is represented as an integer within empirically established limits to guarantee plausible urban expansion scenarios, as advised by Clarke et al. [15] and Dietzel and Clarke [17].

The main steps of the GA include [25], [26]:

The process begins by generating an initial population of individuals. Each individual $x_i$ is a vector:

$$x_i = [d, b, s, sl, r] \quad (1)$$

where d, b, s, sl, and r represent Diffusion, Breed, Spread, Slope, and Road coefficients, respectively. The bounds are set as:

$$d, b, s, r \in [0,50] \text{and} sl \in [0,30] \quad (2)$$

For each individual, the SLEUTH model is run with the given parameters, and a fitness score is computed based on the similarity between simulated and observed urban growth. The fitness function can be formalized as:

$$\text{Fitness}(x_i) = f(\text{SLEUTH}(x_i), \text{Observed}) \quad (3)$$

where f is an evaluation metric such as the Lee-Salle index, kappa statistic, or other agreement measures. In our implementation, a custom score aggregates multiple spatial metrics to guide the search.

The GA employs tournament selection to choose parent individuals for reproduction. In a tournament of size k, k individuals are selected randomly, and the one with the highest fitness is chosen as a parent. This is mathematically represented as:

$$\text{Parent} = \text{argmax}_{x_j \in T} \text{Fitness}(x_j) \quad (4)$$

where T is the tournament subset.

Offspring are generated via uniform crossover, where each gene (parameter) is randomly inherited from one of the two parents with equal probability. If $x_p$ and $x_q$ are parents, the child $x_c$ is defined as:

$$x_c[j] = \begin{cases} x_p[j], & \text{if} u_j < 0.5 \\ x_q[j], & \text{otherwise} \end{cases} \quad (5)$$

where $u_j$ is drawn from a uniform distribution $U(0,1)$ for each gene j.

Mutation introduces random changes to genes with a specified probability μ (here, $\mu = 0.15$). For each gene in the offspring, with probability μ, the gene is replaced by a new random value within its domain:

$$x_c[j] = \begin{cases} \text{Random}(L_j, U_j), & \text{if} v_j < \mu \\ x_c[j], & \text{otherwise} \end{cases} \quad (6)$$

where $L_j$ and $U_j$ are the lower and upper bounds for parameter j, and $v_j \sim U(0,1)$.

To maintain optimal solutions, the leading individuals (elite) are transferred intact to the subsequent generation, while the rest of the new population is populated with progeny. This method safeguards the optimal solutions identified from being compromised by stochastic genetic processes.

The genetic algorithm progresses through generations until a certain number of generations is attained or convergence requirements are satisfied. The individual exhibiting the highest fitness at the conclusion is chosen as the optimal parameter set.

### 3.3.2 SLEUTH

#### 3.3.2.1 Overview

The SLEUTH model functions on a standard two-dimensional grid, with each cell symbolizing a spatial unit capable of transitioning between urban and non-urban states [27]. The state transition of each cell is regulated by deterministic rules applied stochastically, depending on local neighborhood conditions and global growth parameters. The cellular automaton framework can be articulated formally as follows:

$$S_{i,j}^{t+1} = f\left(S_{i,j}^{t}, N_{i,j}^{t}, C, E_{i,j}\right) \quad (7)$$

where $S_{i,j}^{t+1}$ is the state of cell $(i, j)$ at time $t + 1$, $N_{i,j}^{t}$ represents the neighborhood configuration at time $t$, $C = [D, B, S, Sl, R]$ is the vector of growth coefficients, and $E_{i,j}$ represents environmental constraints (slope, exclusions, land use).

The SLEUTH model implements five distinct growth rules that operate sequentially during each simulation year. Each rule is controlled by specific coefficients that regulate the intensity and spatial pattern of urban growth.

#### 3.3.2.2 Diffusion Rule

The diffusion rule models spontaneous urbanization by transforming non-urban cells neighboring established urban zones. A cell is urbanized with a certain probability:

$$P_{diff}(i, j) = \begin{cases} \frac{D}{100} & \text{if} N_{urban}(i, j) > 0 \text{and} \neg S_{i,j}^{t} \\ 0 & \text{otherwise} \end{cases} \quad (8)$$

where D is the diffusion coefficient (0-100), $N_{urban}(i, j)$ is the number of urban cells in the 8-neighborhood of cell $(i, j)$, and $S_{i,j}^{t}$ indicates whether cell $(i, j)$ is already urban at time $t$.

#### 3.3.2.3 Breed Rule

The breed rule produces new growth centers from newly urbanized cells. Each newly urbanized cell can generate further urban growth in its vicinity with a probability:

$$P_{breed}(i, j) = \frac{B}{100} \quad (9)$$

where B is the breed coefficient. The target cell for breeding is randomly selected from the 8-neighborhood of the source cell.

#### 3.3.2.4 Spread Rule

The spread rule applies slope resistance to potential growth sites, filtering candidate cells based on terrain suitability:

$$P_{spread}(i, j) = \max\left(0, \frac{S}{100} - \text{slope\_penalty}(i, j)\right) \quad (10$$

where S is the spread coefficient and the slope penalty is calculated as:

$$\text{slope\_penalty}(i, j) = \frac{Sl}{100} \cdot \frac{1}{1+e^{-(\text{slope}(i,j)-15)/5}} \quad (11)$$

with Sl being the slope resistance coefficient and $\text{slope}(i, j)$ the terrain slope at cell $(i, j)$.

#### 3.3.2.5 Road-Influenced Growth

The road-influenced growth rule simulates urban development attraction to transportation infrastructure:

$$P_{road}(i,j) = \frac{R}{100} \cdot w_{road}(i,j) \quad (12)$$

where R is the road gravity coefficient and $w_{road}(i,j)$ is the road influence weight calculated using Gaussian decay:

$$w_{road}(i,j) = e^{-\alpha \cdot d_{road}(i,j)^2} \quad (13)$$

with $d_{road}(i,j)$ being the Euclidean distance to the nearest road and α being a decay parameter.

#### 3.3.2.6 Self-Modification Mechanism

The self-modification of rules alters control parameters when modeled growth rates are surpassed, so incorporating feedback into the model's behavior. The self-modification system dynamically modifies growth coefficients according to the rate of urban growth in relation to established thresholds.

$$C_{new} = \begin{cases} C \cdot (1 + \text{modifier}) & \text{if growth rate} > \text{critical\_high} \\ C \cdot (1 - \text{modifier}) & \text{if growth rate} < \text{critical\_low} \\ C & \text{otherwise} \end{cases} \quad (14)$$

This adaptive feature enables the model to react to fluctuating growth conditions and sustain realistic urbanization rates across prolonged simulation durations.

#### 3.3.2.7 Calibration Methodology

Conventional SLEUTH calibration utilizes a brute-force method that systematically explores the parameter space throughout many phases. The most notable enhancement for SLEUTH calibration was the transition from a brute force method to a genetic algorithm [14]. The Genetic Algorithm (GA) was employed as an objective way to calibrate the model for three research sites, exhibiting enhanced performance relative to traditional techniques.

#### 3.3.2.8 Genetic Algorithm Implementation

The genetic algorithm optimization seeks to find the optimal coefficient combination that maximizes model fitness. The initial population $P_0$ consists of $N_{pop}$ randomly generated individuals:

$$P_0 = \{C_1, C_2, \ldots, C_{N_{pop}}\} \quad (15)$$

where each individual $C_i$ represents a unique parameter combination within the specified bounds.

The fitness function evaluates model performance using the Optimal SLEUTH Metric (OSM), which combines multiple spatial agreement measures:

$$\text{Fitness}(C) = \text{OSM}(C) = \frac{2 \cdot \text{Lee-Sallee} \cdot \text{Kappa}}{\text{Lee-Sallee} + \text{Kappa}} \quad (16)$$

where Lee-Sallee measures spatial overlap and Kappa assesses classification agreement between simulated and observed urban patterns.

Initialize population $P_0$ with $N_{pop}$ random individuals Evaluate fitness for all individuals in $P_0$ Create new population $P_{new} = \emptyset$ Add elite individuals to $P_{new}$ (elitism) Select parent1 using tournament selection Select parent2 using tournament selection Generate offspring using uniform crossover Apply mutation to offspring Add offspring to $P_{new}$ $P_g = P_{new}$ Evaluate fitness for all individuals in $P_g$ Return best individual from final population.

The genetic algorithm was executed with the subsequent parameters: Population size: 60 people; Number of generations: 80; Mutation rate: 0.15; Tournament size: 3; Elite individuals: 2. Each fitness assessment comprised 50 Monte Carlo iterations to address model stochasticity. The final fitness score denotes the average performance over all iterations, guaranteeing reliable parameter estimation despite the intrinsic randomness in cellular automaton transitions. The model was executed in Python utilizing Numba acceleration for the cellular automaton kernels. Parallel processing was utilized for the evaluation of genetic algorithm populations and Monte Carlo simulations, markedly decreasing computing time relative to conventional brute-force calibration techniques.

### 3.3.2.9 Model Evaluation Metrics

The evaluation of model performance employs various measures that reflect distinct dimensions of spatial concordance between simulated and actual urban patterns.

The Lee-Sallee index quantifies the spatial congruence between simulated and actual metropolitan regions:

$$\text{Lee-Sallee} = \frac{|A_{sim} \cap A_{obs}|}{|A_{sim} \cup A_{obs}|} \quad (17)$$

where $A_{sim}$ and $A_{obs}$ represent simulated and observed urban areas, respectively.

The Kappa coefficient evaluates categorization concordance while considering chance agreement.

$$\text{Kappa} = \frac{P_o - P_e}{1 - P_e} \quad (18)$$

where $P_o$ is the observed agreement and $P_e$ is the expected agreement by chance.

The composite metric integrates multiple spatial measures:

$$\text{Composite} = 0.4 \cdot \text{Edge\_Match} + 0.2 \cdot \text{Fractal\_Similarity} + 0.4 \cdot \text{Lee-Sallee}$$

where Edge_Match measures boundary correspondence and Fractal_Similarity assesses geometric complexity similarity.







Web of Scientists and Scholars: Journal of Multidisciplinary Research

#### 3.3.2.10 Model Validation

Model validation adhered to established SLEUTH protocols by juxtaposing generated urban patterns for a validation year with actual observed development. Testing demonstrated that SLEUTH-GA could calibrate the model with a computational acceleration of 3 to 22 times, while preserving or enhancing calibration accuracy relative to conventional approaches.

## 4. RESULTS AND DISCUSSIONS

### 4.1 Results of Urban Growth Simulation Assessment

The SLEUTH urban growth model, along with genetic algorithm (GA) optimization, attained strong calibration outcomes throughout the three-phase calibration process. The calibration metrics exhibited superior performance, with an average accuracy (S) of 0.965±0.21, signifying an exceptional model fit (Table 3). The Lee-Sallee shape index averaged 0.900±0.05, indicating a robust concordance in spatial pattern alignment between observed and simulated urban expansion. The Kappa coefficient of 0.646±0.14 and the Optimal Sleuth Metric (OSM) of 0.718±0.16 further validated the model's capacity to replicate historical urban development patterns with considerable precision. The GA optimization procedure effectively optimized the SLEUTH growth coefficients from their original values (Table 4). Although the Diffusion and Slope coefficients remained constant at 50, substantial modifications were implemented to other parameters. The Breed coefficient increased from 50 to 100, demonstrating the significance of establishing new spreading centers in the urban growth dynamics of the research area. Correspondingly, the Spread coefficient rose to 100, indicating robust organic development trends in proximity to established urban regions. Conversely, the Road coefficient fell from 50 to 25, indicating that road-influenced growth exerted a less significant influence than previously expected on urban expansion patterns.

Table 3. Average performance of the three-phase calibration of the SLEUTH-GA model.

| Metric | Value |
|---|---|
| S | 0.965±0.21 |
| Lee | 0.900±0.05 |
| Kappa | 0.646±0.14 |
| OSM | 0.718±0.16 |

Table 4. Optimal coefficient values determined by the GA calibration method.

| Coefficient | Initial Value | Optimal Value |
|---|---|---|
| Diffusion | 50 | 50 |
| Breed | 50 | 100 |
| Spread | 50 | 100 |
| Slope | 50 | 50 |
| Road | 50 | 25 |

A visual comparison of actual and simulated urban areas for 2004, 2014, and 2024 demonstrates significant spatial correlation in urban growth trends (Figure 4). In 2004, the model accurately represented the central urban core and the majority of peripheral development zones, while there was an overestimation of sporadic growth in the southern region. The simulation demonstrated notable accuracy in replicating the dense urban structure and primary growth pathways. By 2014, both empirical and simulated maps illustrate considerable urban expansion, with the model precisely forecasting the intensification of the central urban zone and the development of additional growth nodes. The spatial arrangement of urban areas exhibits notable resemblance, with the model adeptly representing both infill development and edge expansion trends. Minor inconsistencies are evident in the southern region, where the model forecasted a marginally more distributed development than what transpired. The 2024 comparison demonstrates the greatest visual alignment, with the model accurately forecasting the merging of once distinct urban areas and the ongoing densification of the urban center. The simulation precisely depicted the trend of northward expansion and the emergence of secondary urban centers. The spatial dispersion of urban expansion demonstrates strong concordance in both compact and leapfrog development patterns.

The model's prediction accuracy shown a steady enhancement over time, with total accuracy rising from 83.45% in 2004 to 91.27% in 2024 (Table 5). This historical trend indicates the model's increasing efficacy in capturing urban growth dynamics as development patterns stabilized and grew more predictable. The Kappa statistics exhibited a comparable trend, increasing from 76.88 in 2004 to 89.22 in 2024, signifying substantial to nearly complete concordance between simulated and actual urban distributions. The 2004 simulation, although the earliest prediction period, attained commendable accuracy levels, with both overall accuracy and Kappa values surpassing recognized benchmarks for effective model performance. The 7.82% enhancement in accuracy from 2004 to 2024 presumably indicates the model's improved capacity to replicate modern urban growth patterns, which are marked by more organized development in accordance with established planning standards.

The gradually improving accuracy metrics indicate that the SLEUTH-GA model successfully assimilated and replicated the fundamental urban growth dynamics in the studied area. The elevated Breed and Spread coefficients suggest that urban expansion was predominantly propelled by organic growth and peripheral expansion rather than development affected by transportation infrastructure. This finding corresponds with the observed urban patterns indicating substantial organic expansion surrounding existing urban regions and the formation of new urban clusters. The comparatively low standard deviations in the calibration measures (notably Lee-Sallee at ±0.05) indicate the model's stability and consistency over various calibration iterations. The OSM value of 0.718±0.16 indicates a balanced optimization across many development measures, ensuring the model encompasses multiple facets of urban growth dynamics rather than focusing on a singular element. The model's enhanced performance in recent years (2024) relative to previous times indicates its specific aptitude for simulating current urban growth patterns. This enhancement can be ascribed to increasingly regulated urban development in recent years, rendering growth patterns more predictable and amenable

to modeling. The effective calibration and elevated validation accuracies demonstrate that the SLEUTH-GA integration offers a dependable framework for simulating urban growth in the study area and maybe for forecasting future urban expansion scenarios.


Figure 4. Comparison of the actual and simulated urban areas in Al-Sulaymaniyah City for the validation years 2004, 2014, and 2024.







Web of Scientists and Scholars: Journal of Multidisciplinary Research

Table 5. Accuracy assessment of the predicted urban areas based on data from 2004-2024.

| Year | Overall Accuracy | Kappa |
|---|---|---|
| 2004 | 83.45 | 76.88 |
| 2014 | 88.63 | 85.73 |
| 2024 | 91.27 | 89.22 |

### 4.2 Results of Urban Growth Prediction

The SLEUTH-GA model forecasted significant urban growth from 1995 to 2034, with the total urban area rising from 143.72 km² to 878.20 km² (Figure 5). This indicates a cumulative expansion of 734.48 km² over the 39-year simulation period, equating to a growth rate of 511.1%. The mean annual urban expansion was determined to be 18.83 km²/year, while the growth trajectory displayed a non-linear pattern typical of urban development dynamics.

The simulated urban maps from 1995 to 2034 demonstrate the gradual amalgamation of urban areas into a more unified urban structure. From 1995 to 2000, urban expansion predominantly manifested as peripheral growth surrounding the established urban core, with minimal leapfrog development. The decade from 2000 to 2010 experienced rapid and fragmented growth, characterized by the emergence of new urban clusters, especially in the northwest and southeast peripheries. A notable geographical transition transpired between 2010 and 2020, marked by infill development that linked hitherto separated metropolitan areas. This phase signifies a transition from extensive to concentrated urban growth patterns. The predictions for 2020-2034 indicate ongoing densification with restricted peripheral expansion, implying a mature urban system nearing its growth limits.

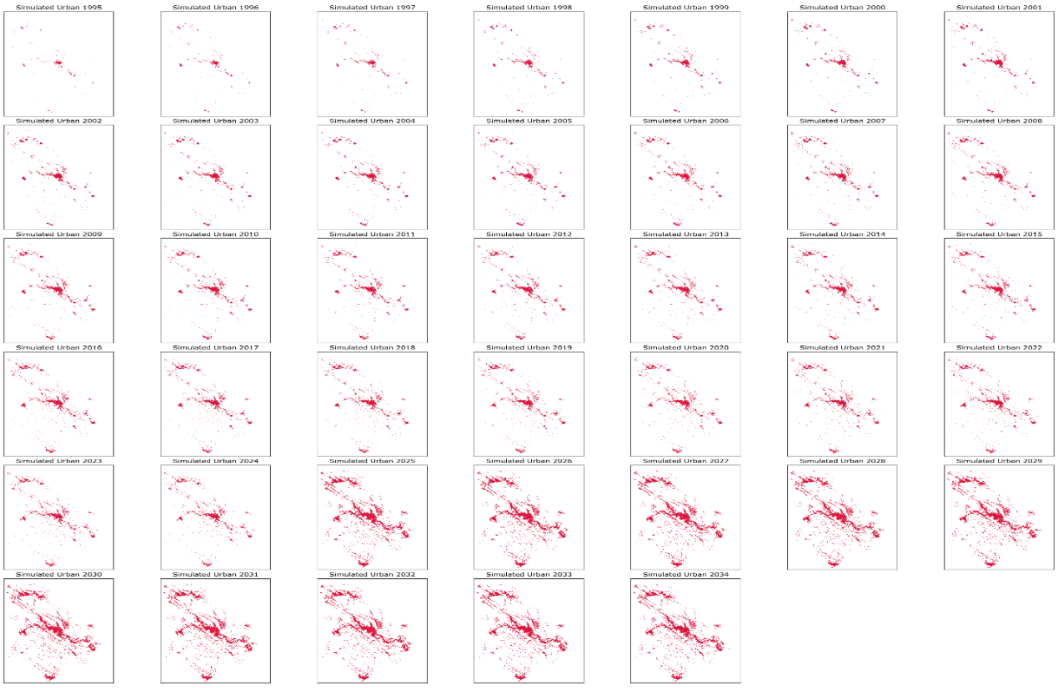


Figure 5. Simulated urban growth for Al-Sulaymaniyah City from 1995 to 2034.

The temporal growth curve exhibits a characteristic S-shaped trajectory, marked by swift expansion in the initial decades (1995-2010) at an average rate of 23.84 km²/year, succeeded by a steady deceleration. The growth rate significantly declined post-2020, with an annual average expansion of merely 5.79 km²/year from 2020 to 2034. This deceleration indicates impending space limitations, governmental measures, or inherent growth restrictions as the metropolitan region evolves. The analysis of the annual growth rate indicates certain phases in the dynamics of urban expansion (Figure 6). The interval from 1995 to 2000 had the most significant growth rates, with yearly expansion surpassing 35 km²/year. The rapid initial expansion subsequently stabilized at around 20 km²/year from 2000 to 2010, before further diminishing to below 10 km²/year post-2015. The anticipated growth from 2025 to 2034 indicates a sustained decline, with annual expansion rates declining to below 3 km² per year. The asymptotic behavior indicates that the urban region is nearing a saturation point, potentially due to geographic limitations, governmental measures, or a reduction in available developable land. The model forecasts a near-stabilization of urban expansion by 2034, with the overall urban area attaining 878.20 km².

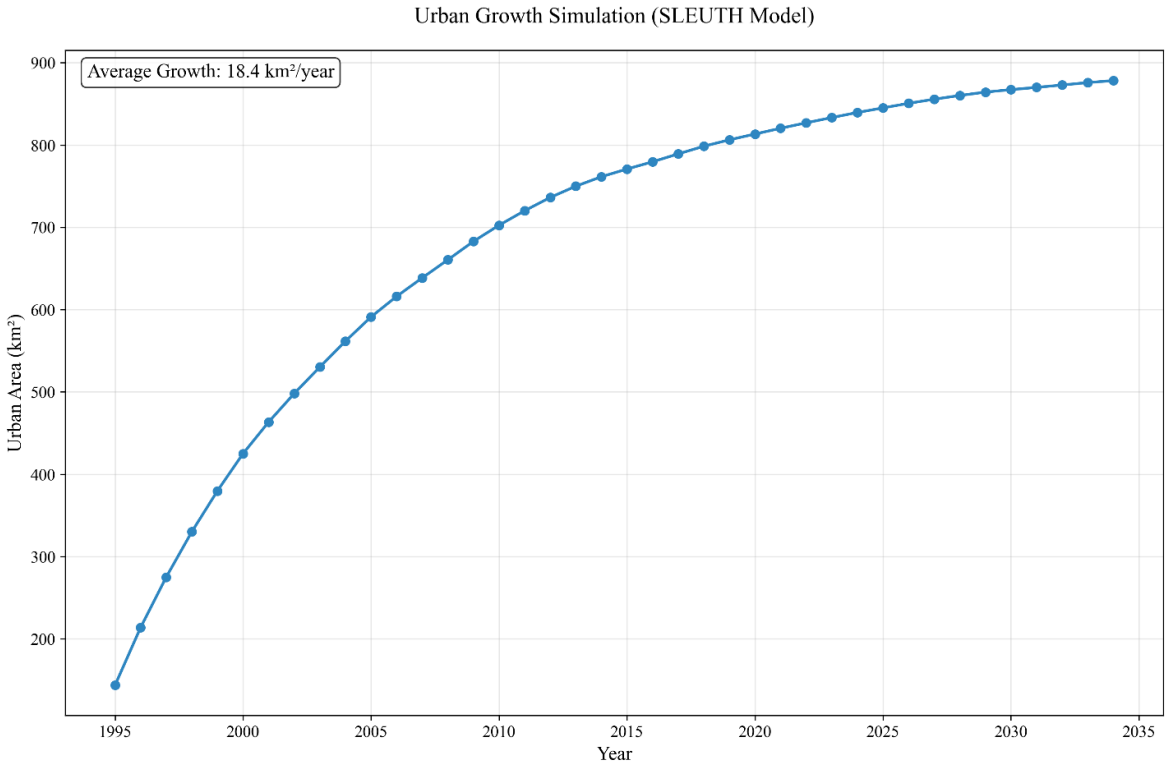


Figure 6. The temporal growth curve of the urban area in Al-Sulaymaniyah city (1995-2034).

The directional analysis indicates significant regional variability in urban growth patterns (Figure 7). The northwest (NW) sector became the principal growth corridor, increasing from 41.46 km² in 1995 to 269.23 km² by 2034, signifying a 549% expansion. The northwestern tendency in urban development remained consistent throughout the simulated period, with the NW sector comprising 30.7% of the total urban area by 2034. The southeast (SE) sector

demonstrated the second-highest growth, rising from 29.88 km² to 160.92 km², succeeded by the southern (S) direction, which expanded from 10.85 km² to 104.06 km². The western (W) sector saw significant growth from 23.48 km² to 130.49 km², indicating the development of a secondary growth axis. In contrast, the eastern (E) and southwestern (SW) sectors saw the most limited growth, increasing to merely 36.78 km² and 30.95 km², respectively, by 2034. This restricted eastern expansion presumably indicates geographic limitations or planning regulations that directed development elsewhere. The polar diagram representation accurately illustrates the directional bias, with a pronounced elongation toward the northwest evident. The radial pattern indicates that urban expansion has not occurred uniformly but has instead been directed along particular growth corridors, likely shaped by infrastructure, terrain, or planning laws.

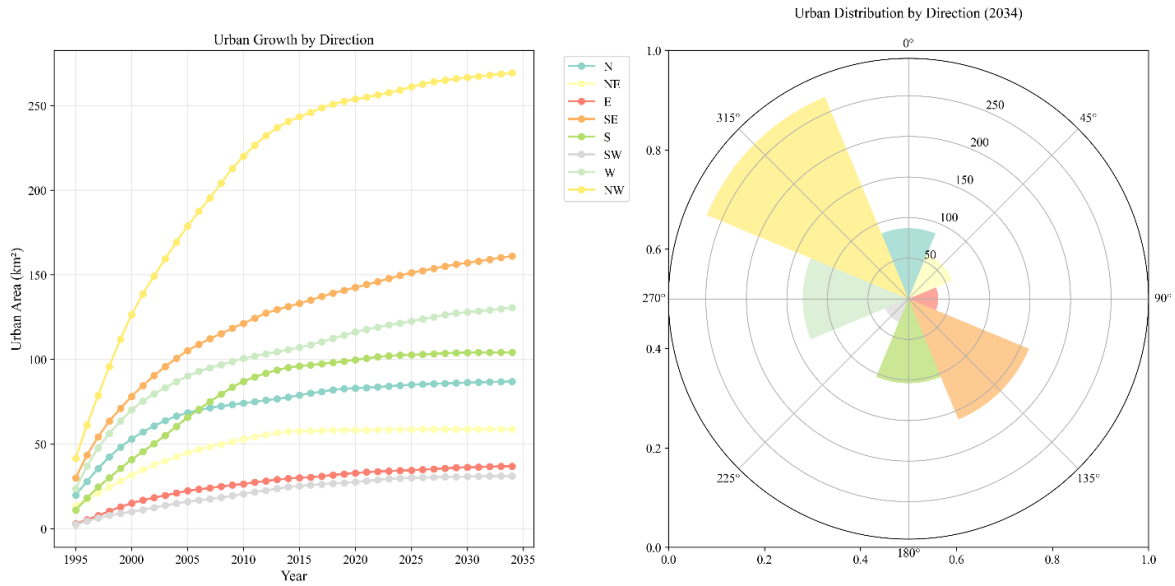


Figure 7. The directional distribution of the urban areas in the study area over the simulation period, 1995-2034.

The correlation analysis between road distance and urban development continually demonstrated unfavorable associations throughout the simulation period, supporting the enduring impact of transportation infrastructure on urban growth patterns. Both Pearson and Spearman correlation coefficients exhibited analogous trends, with Pearson's r values spanning from -0.187 to -0.073 and Spearman's r values ranging from -0.191 to -0.073 (Figure 8). The correlation strength shown a progressive decline over time, with the most pronounced negative correlations recorded in the initial simulation years (1995-2005), when Pearson's r averaged -0.188. This robust initial association suggests that early urban development closely adhered to pre-existing road networks. The link diminished throughout time, attaining -0.073 by 2034, indicating that subsequent urban development became increasingly independent of proximity to main roadways. This temporal trend in correlation coefficients indicates a transformation in the factors driving urban expansion. The initial growth pattern reliant on road infrastructure (1995-2005) likely indicates infrastructure-led development, whereas the diminishing

correlation in subsequent years (2020-2034) implies the rise of alternative factors, including land availability, planning regulations, or economic considerations, as principal determinants of growth. The simulation outcomes yield essential insights for urban planning and policy development. The significant northwestern growth tendency indicates a necessity for improved infrastructure development and service delivery in that area. The diminishing association with road proximity over time suggests that future urban development may necessitate alternative planning methodologies beyond conventional transportation-focused solutions. The anticipated slowdown in growth post-2020 presents a chance to adopt sustainable urban development approaches, as the demand for rapid expansion lessens. The identification of key growth corridors (NW, SE, W) can inform the strategic deployment of resources and the formulation of focused land use plans to successfully control urban expansion while safeguarding critical ecological and agricultural zones in limited directions.

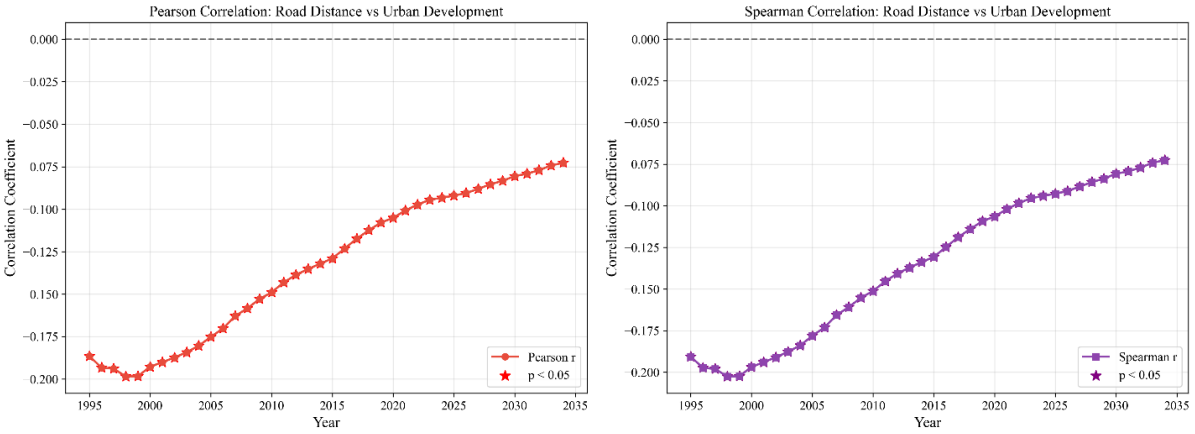


Figure 8. The spatial correlation between the urban areas and distance from roads.

## 5. CONCLUSIONS

This study effectively showcased the amalgamation of genetic algorithm optimization with the SLEUTH urban growth model, yielding a computationally efficient and precise framework for simulating urban expansion in Al-Sulaymaniyah City. The study's methodological breakthrough overcomes significant limits in conventional SLEUTH calibration methods, attaining considerable computing efficiency while preserving exceptional model performance. The GA optimization successfully enhanced growth coefficients, with Breed and Spread parameters attaining their maximum values (100), signifying the predominance of spontaneous growth and edge expansion mechanisms in the urbanization process of the research area. The remarkable land cover categorization accuracy (93%) and elevated Kappa coefficient (0.90) provided a solid basis for urban expansion analysis. The recorded alteration of Al-Sulaymaniyah's terrain, notably the 374% increase in constructed areas over thirty years, illustrates the swift urbanization typical of post-conflict economic advancement in the Kurdistan Region. The model's increasing validation accuracy from 83.45% to 91.27% illustrates its improved capacity to represent current urban dynamics, indicating its specific appropriateness for replicating regulated urban development patterns in contemporary Middle

Eastern cities. Spatial research provided essential insights into directional growth trends, with northwestern expansion prevailing in urban development trajectories. The diminishing association between road proximity and urban expansion over time (r = -0.188 to -0.073) signifies a fundamental transformation in the determinants of urbanization, transitioning from infrastructure reliance to multifaceted development patterns. This discovery has significant implications for urban planning techniques, indicating the necessity to transcend conventional transportation-focused development methods in favor of more holistic planning frameworks that account for many growth variables. The anticipated reduction in growth, with yearly expansion rates decreasing from 35 km²/year to around 3 km²/year by 2034, indicates an impending urban saturation phase. This asymptotic trend poses both obstacles and opportunities for sustainable urban management. The designation of 878.20 km² as the anticipated urban extent for 2034 offers planners essential insights for infrastructure development, service delivery, and environmental conservation initiatives. The study's results had immediate practical implications for urban government in Al-Sulaymaniyah and comparable fast expanding communities. The significant directional growth bias requires focused infrastructure investments in northwestern corridors and the implementation of conservation measures in limited eastern areas. The recorded recovery of agricultural land, with cropland increasing by 54% compared to 1994 levels, illustrates effective land rehabilitation that necessitates safeguarding via suitable zoning restrictions.

Notwithstanding these achievements, specific limits warrant recognition. The model's dependence on historical development trends may inadequately account for anticipated shocks from developing technology, climate change effects, or significant policy changes. Furthermore, the static characteristic of the exclusion layer may fail to represent the developing goals of environmental protection or the fluctuating values of agricultural land. Future study should investigate dynamic exclusion layers that adapt to temporal variations in environmental and regulatory restrictions. The incorporation of socioeconomic data, especially demographic forecasts and economic metrics, could improve model complexity. Examining the application of the GA-SLEUTH paradigm to additional swiftly urbanizing cities in the Middle East would confirm its wider utility. Additionally, integrating urban growth forecasts with climate change scenarios may yield essential insights for resilient urban planning in semi-arid areas. This comprehensive modeling technique provides a solid basis for evidence-based urban planning, aiding in the achievement of sustainable development objectives in swiftly evolving urban environments.

## REFERENCES

[1]U. N. Habitat, International guidelines on urban and territorial planning. Nairobi: United Nations Human Settlements Programme, 2015.

[2]K. C. Clarke, “Land use change modeling with sleuth: Improving calibration with a genetic algorithm,” Geomatic approaches for modeling land change scenarios, pp. 139–161, 2018.

[3]G. Chaudhuri and K. C. Clarke, "Modeling an Indian megalopolis – A case study on adapting SLEUTH urban growth model," Computers, Environment and Urban Systems, vol. 77, p. 101358, 2019.
[4]K. C. Clarke and J. M. Johnson, "Calibrating SLEUTH with big data: Projecting California's land use to 2100," Computers, Environment and Urban Systems, vol. 83, p. 101525, 2020.
[5]S. H. A. Jarah, B. Zhou, R. J. Abdullah, Y. Lu, and . W. Yu, "Urbanization and urban sprawl issues in city structure: A case of the Sulaymaniah Iraqi Kurdistan Region," Sustainability, vol. 11, no. 2, p. 485, 2019.
[6]V. Kumar and S. Agrawal, "Urban modelling and forecasting of landuse using SLEUTH model," International Journal of Environmental Science and Technology, vol. 20, no. 6, pp. 6499–6518, 2023.
[7]A. Saxena and M. K. Jat, "Capturing heterogeneous urban growth using SLEUTH model," Remote Sensing Applications: Society and Environment, vol. 13, pp. 426–434, 2019.
[8]B. Ding, Z. Yang, and T. Liu, "Urban future prediction based on genetic algorithm-back propagation neural network," in Fourth International Conference on Intelligent Traffic Systems and Smart City (ITSSC 2024), H. Chen and W. Shangguan, Eds., Xi'an, China: SPIE, Jan. 2025, p. 73. doi: 10.1117/12.3050833.
[9]G. R. Faqe, P. A. Ibrahim Saied, and H. M. Hameed, "Urban Growth prediction using cellular automata Markov: a case study using Sulaimaniya city in the Kurdistan Region of North Iraq," IISTE Humanit Soc Sci, vol. 6, pp. 108–118, 2016.
[10] M. D. Clarke-Lauer and K. C. Clarke, "Evolving simulation modeling: Calibrating SLEUTH using a genetic algorithm," in Proceedings of the 11th International Conference on GeoComputation, London, UK (Vol, Jul. 2011, pp. 20–22.
[11] B. Dey and P. Sharma, "A comprehensive review of urban growth studies and predictions using the Sleuth model," The Scientific Temper, vol. 15, no. 02, pp. 2333–2341, 2024.
[12] E. Foroutan and M. R. Delavar, "Urban growth modeling using genetic algorithms and cellular automata; A case study of Isfahan Metropolitan Area, Iran," Proceedings of the GIS Ostrava, pp. 23–25, 2012.
[13] X. Li and L. Parrott, "An improved Genetic Algorithm for spatial optimization of multi-objective and multi-site land use allocation," Computers, Environment and urban systems, vol. 59, pp. 184–194, 2016.
[14] D. Liu, K. C. Clarke, and N. Chen, "Integrating spatial non-stationarity into SLEUTH for urban growth modelling: A case study in the Wuhan metropolitan area," Computers, Environment and Urban Systems, vol. 84, p. 101545, 2020.
[15] K. C. Clarke, S. Hoppen, and L. Gaydos, "A self-modifying cellular automaton model of historical urbanization in the San Francisco Bay area," Environment and planning B: Planning and design, vol. 24, no. 2, pp. 247–261, 1997.
[16] E. A. Silva and K. C. Clarke, "Calibration of the SLEUTH urban growth model for Lisbon and Porto, Portugal," Computers, environment and urban systems, vol. 26, no. 6, pp. 525–552, 2002.

[17] C. Dietzel and K. C. Clarke, "Toward optimal calibration of the SLEUTH land use change model," Transactions in GIS, vol. 11, no. 1, pp. 29–45, 2007.
[18] J. Jafarnezhad, A. Salmanmahiny, and Y. Sakieh, "Subjectivity versus objectivity: comparative study between brute force method and genetic algorithm for calibrating the SLEUTH urban growth model," Journal of urban planning and development, vol. 142, no. 3, p. 05015015, 2016.
[19] S. Berberoglu, A. Akın, and K. C. Clarke, "Cellular automata modeling approaches to forecast urban growth for Adana, Turkey: A comparative approach," Landscape and Urban Planning, vol. 153, pp. 11–27, 2016.
[20] X. Wu, Y. Hu, H. S. He, R. Bu, J. Onsted, and F. Xi, "Performance Evaluation of the SLEUTH Model in the Shenyang Metropolitan Area of Northeastern China," Environ Model Assess, vol. 14, no. 2, pp. 221–230, Apr. 2009, doi: 10.1007/s10666-008-9154-6.
[21] W. Yi and B. He, "Applying SLEUTH for Simulating Urban Expansion of Beijing," in 2009 International Forum on Information Technology and Applications, Chengdu, China: IEEE, May 2009, pp. 652–656. doi: 10.1109/IFITA.2009.543.
[22] U. A. Saulawa, Y. Ibrahim, and A. Bello, "Assessing the suitability of the SLEUTH cellular automata model for capturing heterogeneous urban growth in developing cities: A case study in Northern Nigeria," Heliyon, vol. 10, no. 17, 2024.
[23] C. A. Jantz, S. J. Goetz, and M. K. Shelley, "Using the SLEUTH urban growth model to simulate the impacts of future policy scenarios on urban land use in the Baltimore-Washington metropolitan area," Environment and Planning B: Planning and Design, vol. 31, no. 2, pp. 251–271, 2004.
[24] Y. Zhou, A. C. G. Varquez, and M. Kanda, "High-resolution global urban growth projection based on multiple applications of the SLEUTH urban growth model," Scientific Data, vol. 6, p. 34, 2019.
[25] D. E. Goldberg, "Genetic algorithm in search, optimization and machine learning, addison," esley Publishing Company, R eading, MA, vol. 1, no. 98, p. 9, 1989.
[26] M. Batty, Cities and Complexity: Understanding Cities with Cellular Automata, Agent-Based Models, and Fractals. MIT Press, 2007.
[27] G. Chaudhuri and K. C. Clarke, "The SLEUTH land use change model: A review," The International Journal of Environmental Resources Research, vol. 1, no. 1, pp. 88–105, 2013.